AD_____

Award Number: DAMD17-98-1-8224

TITLE: Applications of a Novel Nucleic Acid Detection Method in Breast Cancer Analysis of Overexpression of HER-2/neu and FAK

PRINCIPAL INVESTIGATOR: Herbert Thorp, Ph.D.

CONTRACTING ORGANIZATION: University of North Carolina
Chapel Hill, North Carolina 27599-1350

REPORT DATE: July 2000

TYPE OF REPORT: Annual

PREPARED FOR: U.S. Army Medical Research and Materiel Command
Fort Detrick, Maryland 21702-5012

REPORT DOCUMENTATION PAGE

OMB No. 074-0188

1. AGENCY USE ONLY (Leave blank)	2. REPORT DATE	3. REPORT TYPE AND DATES COVERED
	July 2000	Annual (1 Jul 99 - 30 Jun 00)

4. TITLE AND SUBTITLE
Applications of a Novel Nucleic Acid Detection Method in Breast Cancer Analysis of Overexpression of HER-2/neu and FAK

5. FUNDING NUMBERS
DAMD17-98-1-8224

6. AUTHOR(S)
Herbert Thorp, Ph.D.

7. PERFORMING ORGANIZATION NAME(S) AND ADDRESS(ES)
University of North Carolina
Chapel Hill, North Carolina 27599-1350

E-MAIL:
holden@unc.edu

8. PERFORMING ORGANIZATION REPORT NUMBER

9. SPONSORING / MONITORING AGENCY NAME(S) AND ADDRESS(ES)
U.S. Army Medical Research and Materiel Command
Fort Detrick, Maryland 21702-5012

10. SPONSORING / MONITORING AGENCY REPORT NUMBER

11. SUPPLEMENTARY NOTES

12a. DISTRIBUTION / AVAILABILITY STATEMENT
Approved for public release; distribution unlimited

12b. DISTRIBUTION CODE

13. ABSTRACT *(Maximum 200 Words)*

The routine, low-cost detection of genetic material is an important step in translating the advances in cancer genetics to therapeutics and diagnosis. In this study, metal oxide electrodes and a solution oxidant of DNA have been used to detect electrochemically the products of the polymerase chain reaction (PCR) performed on mRNA from the HER-2 gene in BT-474 cancer cells. This method can be used to detect as little as 500 attomoles of DNA quickly and at low cost. The technique has recently been expanded to include detection of the size of PCR fragments, which is reflected in the size of the measured currents. This technique has been applied to sequences that are particularly difficult to size and amplify, such as trinucleotide repeats.

14. SUBJECT TERMS	15. NUMBER OF PAGES
Breast Cancer	21
	16. PRICE CODE

17. SECURITY CLASSIFICATION OF REPORT	18. SECURITY CLASSIFICATION OF THIS PAGE	19. SECURITY CLASSIFICATION OF ABSTRACT	20. LIMITATION OF ABSTRACT
Unclassified	Unclassified	Unclassified	Unlimited

FOREWORD

Opinions, interpretations, conclusions and recommendations are those of the author and are not necessarily endorsed by the U.S. Army.

N/A Where copyrighted material is quoted, permission has been obtained to use such material.

___ Where material from documents designated for limited distribution is quoted, permission has been obtained to use the material.

N/A Citations of commercial organizations and trade names in this report do not constitute an official Department of Army endorsement or approval of the products or services of these organizations.

N/A In conducting research using animals, the investigator(s) adhered to the "Guide for the Care and Use of Laboratory Animals," prepared by the Committee on Care and use of Laboratory Animals of the Institute of Laboratory Resources, national Research Council (NIH Publication No. 86-23, Revised 1985).

X For the protection of human subjects, the investigator(s) adhered to policies of applicable Federal Law 45 CFR 46.

N/A In conducting research utilizing recombinant DNA technology, the investigator(s) adhered to current guidelines promulgated by the National Institutes of Health.

N/A In the conduct of research utilizing recombinant DNA, the investigator(s) adhered to the NIH Guidelines for Research Involving Recombinant DNA Molecules.

N/A In the conduct of research involving hazardous organisms, the investigator(s) adhered to the CDC-NIH Guide for Biosafety in Microbiological and Biomedical Laboratories.

7/16/2000

PI - Signature Date

Table of Contents

Introduction

The proposal "Applications of a Novel Nucleic Acid Detection Method in Breast Cancer: Analysis of Overexpression of HER-2/neu and FAK" is aimed at utilizing new biosensors based on guanine electron transfer to quantitate messenger RNA for breast cancer genes. The biosensors are based on a scheme involving abstraction of electrons from the guanines of immobilized RNA to generate a signature current for a specific gene. The purpose of the proposed research is to demonstrate that the guanine electron transfer technology can be used to detect overexpressed RNAs in real biological samples. The scope involves detection of the mRNAs for HER-2/neu and FAK, which are both known markers of breast cancer, in samples generated by PCR amplification, reverse transcription, or direct RNA extraction. This report describes experiments that led to completion of the first task in the approved Statement of Work -- detection of the HER-2/neu gene from BT-474 cells using PCR amplification. Changes in the immobilization strategy were required that suggest adjustments in the future tasks that have been sent to the contract specialists (Cheryl Lowery, Steve Krosnick) under separate cover.

Body

The sensing technology used in the research is based on electron transfer from guanine in immobilized nucleic acids to a solid electrode.(*1*) The electron transfer is mediated by a soluble small mediator, $Ru(bpy)_3^{2+}$ (bpy = 2,2'-bipyridine), which greatly enhances the current generated from immobilized nucleic acids by accelerating the electron transfer reaction.(*2, 3*) The mediator is oxidized at the electrode (eq 1) and then abstracts an electron from guanine to regenerate the reduced form and complete a catalytic cycle. In the absence of the mediator, the direct abstraction of electrons from guanine is extremely slow and produces little or no signal.

$$Ru(bpy)_3^{2+} \rightarrow Ru(bpy)_3^{3+} + e^- \quad (1)$$

$$Ru(bpy)_3^{3+} + G \rightarrow Ru(bpy)_3^{2+} + G^+ \quad (2)$$

The sensing strategy is based on immobilizing probes to the electrode where inosine is substituted for guanine, prohibiting electron transfer according to eq 2.(*4, 5*) When the silent inosine probe is hybridized to a large, guanine-containing DNA or RNA target, high concentrations of guanine are generated at the electrode and a large current is generated via the cycle shown in eqs 1 and 2.

Central to using the mediated electron transfer strategy is a means for immobilizing inosine-substituted probes on solid electrodes. We have reported a number of such strategies, and the original proposal called for a promising method we had developed that utilized poly(ethylene terephthalate) (PET) membranes attached to indium tin oxide (ITO) electrodes.(*4*) We have tested this strategy on biological samples and have found problems with the reproducibility that were not apparent with the model samples. We have therefore developed a new strategy based on direct adsorption for detecting PCR products that was described in the previous annual report and been published (*6*). Here we describe use of this protocol to detect the size of PCR fragments in a very simple manner. For testing this strategy, we have used triplet repeat sequences,

which can be generated in controlled sizes. Detection of triplet repeats could be relevant to determining microsatellite expansion (*7*) or the ability to distinguish the size of DNA fragments could be useful in distinguishing multiple PCR fragments.

Results - PCR. *(CTG·CAG)$_n$.* Fragments of (CTG·CAG)$_n$ trinucleotide repeat PCR products were synthesized using a nonconventional PCR protocol that utilizes two complementary oligonucleotides, (CTG)$_{20}$ and (CAG)$_{20}$, both as template and primer (*8*). These oligonucleotides hybridize with different degrees of overlap. Pairs with a 5' overhang become templates for extension by DNA polymerase, and each cycle of PCR increases the average length of the population. This procedure leads to a heterogeneous population of PCR products, shown on the gel in Figure 1. Quantitation of DNA in the gel gives the average lengths of PCR products to be 450, 700, 1200, and 2500 base pairs. The size heterogeneity increases for longer repeats, as would be expected for this protocol.

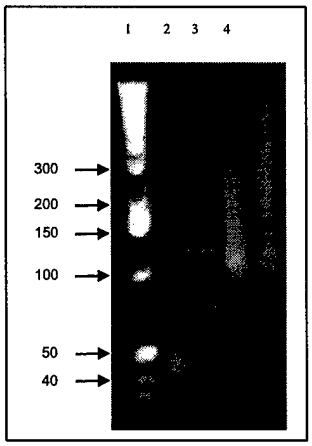

Figure 1. Agarose gel showing the sizes of (CTG·CAG)$_n$ PCR products. Lanes: **1** 1 kb DNA ladder, **2** 450 bp, **3** 700 bp, **4** 1200 bp, **5** 2500 bp. Average sizes were estimated by drawing histograms using AAB 1D Main software

Specific PCR conditions used to synthesize (CTG·CAG)$_n$ repeats of different average lengths are summarized in the experimental section. The most important variables are the extension time and the concentration of mononucleotide triphosphates. According to the published protocol (*8*), the extension time for the 450-bp product was sequentially increased from 1.5 min to 5 min to allow for gradual increase in the length of generated DNA fragments. This strategy, however, did not afford large repeats in our study. Instead, longer extension times (3.5 min for 700-bp product and 5 min for 1200-bp product) were used for all 25 cycles of PCR. The 2500-bp product was synthesized by increasing the number of cycles with 5-minute extension time to 29 and including a final 9-minute extension.

(CGG·CCG)$_n$. Polynucleotides containing (CGG·CCG)$_n$ repeats were synthesized using the same strategy from (CGG)$_{20}$ and (CCG)$_{20}$ oligonucleotides. Several modifications to the procedure had to be made to accommodate the increase in the GC content from 67% to 100%. Higher GC content leads to more secondary structure (*9*) and consequently more polymerase pauses, making synthesis of longer products a challenging

task. Only two PCR products were generated, one with the average length of 400 bp and the other with the average length of 1800 bp (Figure 2). The first modification to the procedure was a decrease in the annealing temperature from 65°C used for $(CTG{\cdot}CAG)_n$ to 50°C. Lower annealing temperature most likely allows for more mispairing events, leading to more 5' overhangs and therefore synthesis of longer products by DNA polymerase. Specific PCR conditions used to synthesize $(CGG{\cdot}CCG)_n$ repeats are summarized in the experimental section. In addition to more cycles, higher concentrations of mononucleotide triphosphates and Mg^{2+} were necessary to synthesize the full mutation range repeat.

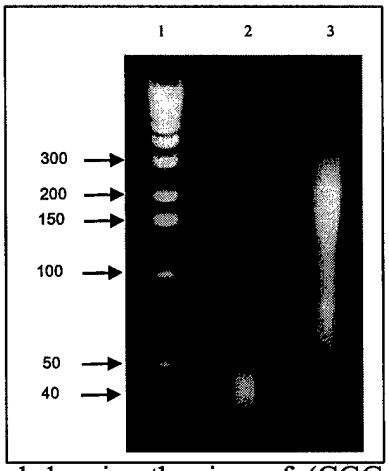

Figure 2. Agarose gel showing the sizes of $(CGG{\cdot}CCG)_n$ PCR products. Lanes: **1** 1 kb DNA ladder, **2** 400 bp, **3** 1800 bp. Average sizes were estimated by drawing histograms using AAB 1D Main software

Immobilization. *$(CTG{\cdot}CAG)_n$.* The $(CTG{\cdot}CAG)_n$ PCR products were immobilized on tin-doped indium oxide (ITO) electrodes according to a method that has recently been developed in our laboratory (*6*). In this protocol, DNA is precipitated from the 9:1 solution of dimethylformamide (DMF) and 100 mM sodium acetate, pH 6.8 by incubation in a constant humidity chamber for 1 hr. Extensive washing with water and salt removes excess DNA that is not immobilized strongly on the surface. The $(CTG{\cdot}CAG)_{10}$ oligonucleotide was immobilized in the same manner. The DNA is most likely attached to the surface as single strands by means of the phosphate backbone. The extents of electrode modification for DNA molecules containing different number of repeats were determined by phosphorimagery of electrodes that have been modified with [^{32}P]-labeled DNA. Quantification was performed phosphorimagery as we have previously described (*6*) and comparison to a control electrode that was not been subjected to washing steps and therefore contained 500 fmol strand DNA.

Average amounts of immobilized DNA are similar for different length repeats. Between 8 and 9% of total DNA that was incubated on the electrode is immobilized regardless of DNA length. Two factors most likely play a role in immobilization efficiency of DNA fragments of different lengths. First, longer DNA fragments are expected to be immobilized with higher efficiency due to the presence of larger number of phosphate groups on each individual strand; in the initial studies, the immobilization efficiency was very high for sonicated calf-thymus DNA samples whose average length

was 1000-3000 bp. Second, shorter pieces occupy a smaller area so a larger number of strands of shorter PCR products could precipitate. Although this is especially true for small $(CTG{\cdot}CAG)_{10}$ oligonucleotides, the number of strands of the immobilized oligonucleotide is still comparable to that of the longer PCR products. These two opposing effects apparently counteract each other during the relatively short incubation time of 1 hour.

$(CGG{\cdot}CCG)_n$. Polynucleotides containing the $(CGG{\cdot}CCG)_n$ repeats were immobilized on the ITO surface in a similar fashion. This sequence was harder to immobilize, probably because sequences with 100% GC content exhibit more non-canonical secondary structure than the $(CTG{\cdot}CAG)_n$ repeat (*9*). Two adjustments had to be made to precipitate enough DNA for voltammetry experiments. The incubation time was increased to 6 h because the quantity of PCR products immobilized during the one-hour incubation time was not sufficient to observe current enhancement in cyclic voltammetry. Dimethylformamide presumably denatures the non-canonical secondary structures over a longer period of time, thereby allowing for more strands of DNA to be deposited on the electrode surface. Larger quantities of DNA were immobilized during the increased time but the amounts were inconsistent from experiment to experiment. To increase the reproducibility, the Alconox wash was omitted in the electrode cleaning procedure. Phosphates in the soap probably interact with the ITO surface, leaving a variable number of available sites where DNA can be immobilized. This did not present a problem in the initial experiments on this system nor in the immobilization of the $(CTG{\cdot}CAG)_n$ repeat, but appears to be significant only when high degree of non-canonical secondary structure is present in DNA fragments to be immobilized.

Quantities of the immobilized CGG repeat were also determined by phosphorimagery. Three important points need to be made in regard to the amounts of immobilized DNA. First, the DNA solution that is applied to the electrode does not spread over the entire surface area, because omission of the soap wash renders the electrode surface less hydrophobic. To increase the area covered, the total solution volume was increased to 30 μL, which increases the amount of DNA applied to the surface to 750 fmol strand. It is important to cover enough electrode area to insure that the portion of the electrode sampled by cyclic voltammetry is modified with reproducible amounts of DNA. Second, in contrast to the $(CTG{\cdot}CAG)_n$ repeat, the amounts of different length DNA fragments vary considerably. The $(CGG{\cdot}CCG)_{20}$ oligonucleotide is immobilized with the greatest efficiency, followed by the 400 bp PCR product, which is followed by the 1800 bp PCR product. This effect is most likely attributed to the long incubation time. More strands of shorter fragments will be immobilized if given enough time because they occupy a smaller area. Third, between 15 and 60% of $(CGG{\cdot}CCG)_n$ strands are immobilized on the surface, which is 3-10 times more than $(CTG{\cdot}CAG)_n$ fragments. This is a direct consequence of the longer incubation time and is important because, as it will be discussed below, more $(CGG{\cdot}CCG)_n$ strands are necessary to see current enhancement in voltammetry experiments.

Electrochemical analysis. *$(CTG{\cdot}CAG)_n$.* Electrochemical detection of $(CTG{\cdot}CAG)_n$ repeats was achieved by $Ru(bpy)_3^{2+}$-mediated voltammetry at high scan rates. High scan rates are essential in the case when DNA is immobilized on the electrode surface and catalyst is in solution. This is because the thickness of the diffusion

layer decreases with increasing scan rate, allowing the catalyst molecules to be in close proximity of DNA. This in turn increases the number of catalytic cycles and leads to more current enhancement. A representative set of cyclic voltammograms of $(CTG{\cdot}CAG)_n$-modified ITO electrodes is shown in Figure 3A. Current enhancement is observed for all the samples ranging in length from 30 to 2500 base pairs with the amount of current enhancement increasing with the length of the repeat.

The amount of current enhancement scales linearly with the length of the repeat, as shown in Figure 3B. This result is in close agreement with our previous solution electrochemical studies on short trinucleotide repeat oligonucleotides where we also observed a linear increase in current response as the length of the repeat increased (*10*). This result is expected since the number of guanines per repeat is fixed and therefore the length of the repeat is directly proportional to guanine concentration. The linear increase is also in agreement with surface electrochemical studies performed on PCR products where the current increases with the increasing amount of immobilized DNA (*6*). Shown in Figure 3C is the plot of current normalized to the number of strands immobilized as the function of DNA length. Normalized current increases in the same manner as the raw current, which is not surprising since similar amounts of DNA are present on the electrode surface for different length DNA molecules.

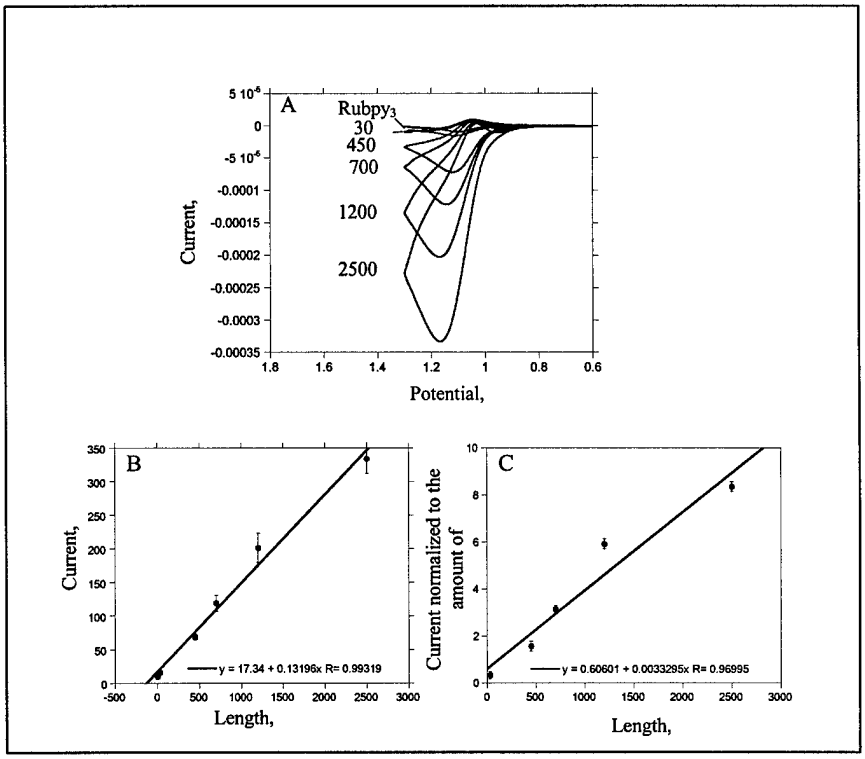

Figure 3. Electrochemical data for $(CTG{\cdot}CAG)_n$ oligonucleotide and PCR products. **(A)** Respresentative set of cyclic voltammograms of DNA-modified ITO electrodes with 25 uM $Ru(bpy)_3^{2+}$ in 50 mM sodium phosphate, pH 7 taken at 10 V/sec. **(B)** Average peak current as a function of DNA length. Each point represents a mean value with one standard deviation of five electrodes. **(C)** Peak current from (B) normalized to the amount of DNA immobilized.

(CGG·CCG)$_n$. The (CGG·CCG)$_n$ repeats were detected electrochemically analogously to the (CTG·CAG)$_n$ repeats. A representative set of cyclic voltammograms is shown in Figure 4A. The amount of current enhancement observed for the 400-bp PCR product is slightly higher than that for the (CTG·CAG)$_{450}$, which is expected from the 50% guanine content of the (CGG·CCG)$_n$ repeat compared to the 33% guanines in the (CTG·CAG)$_n$ fragments. However, this is not the case for the full mutation range repeat where the current enhancement observed for (CGG·CCG)$_{1800}$ is comparable to that for (CTG·CAG)$_{2500}$. This discrepancy is probably due to the saturation of current response for the (CGG·CCG)$_{1800}$ fragment, which is also apparent in the shape of the voltammogram compared to that of the (CTG·CAG)$_{2500}$ repeat. In the initial studies on this reaction, highly sigmoidal voltammograms were observed at maximal levels of detectable DNA (*6*). Another line of evidence for this explanation comes from solution electrochemical studies on polymeric DNA molecules, where we have also seen the shape of the voltammogram become more sigmoidal as the amount of DNA is increased (*3*).

The plot of current as a function of DNA length for (CGG·CCG)$_n$ is shown in Figure 4B. The most important observation in regard to the plot in Figure 6B is the reproducibility of electrochemical response. Three sets of data collected on different days and with different batches of ITO electrodes are in excellent agreement with each other. A modification to the immobilization procedure made to achieve this level of reproducibility was the omission of the Alconox step in the electrode cleaning procedure. As discussed above, phosphates in the soap probably interact with the ITO electrode, thereby rendering the number of available sites on the electrode surface variable. The variable number of open sites not only decreases the reproducibility of the amounts of immobilized DNA fragments but also affects the interaction of the catalysts with the electrode surface. This heterogeneous electron-transfer step is crucial for the catalytic current to be observed, and variations in the number of sites where ruthenium can exchange electrons with the electrode leads to variable amounts of current enhancement.

Shown in Figure 4C is the plot of current normalized to the amount of immobilized DNA as a function of DNA size. As with the (CTG·CAG)$_n$ repeat, the normalized current increases linearly with repeat length. However, the overall amounts of normalized current are smaller, ranging from 0.1 to ~3 μA/fmol strand as opposed to between 0.1 and ~ 8 μA/fmol strand for (CTG·CAG)$_n$ fragments. It is apparently more difficult to extract electrons from (CGG·CCG)$_n$ repeats so higher quantities of immobilized DNA were necessary to observe current enhancement. This situation probably occurs because more guanines are involved in non-canonical secondary structures, which causes them to extend further from the electrode surface.

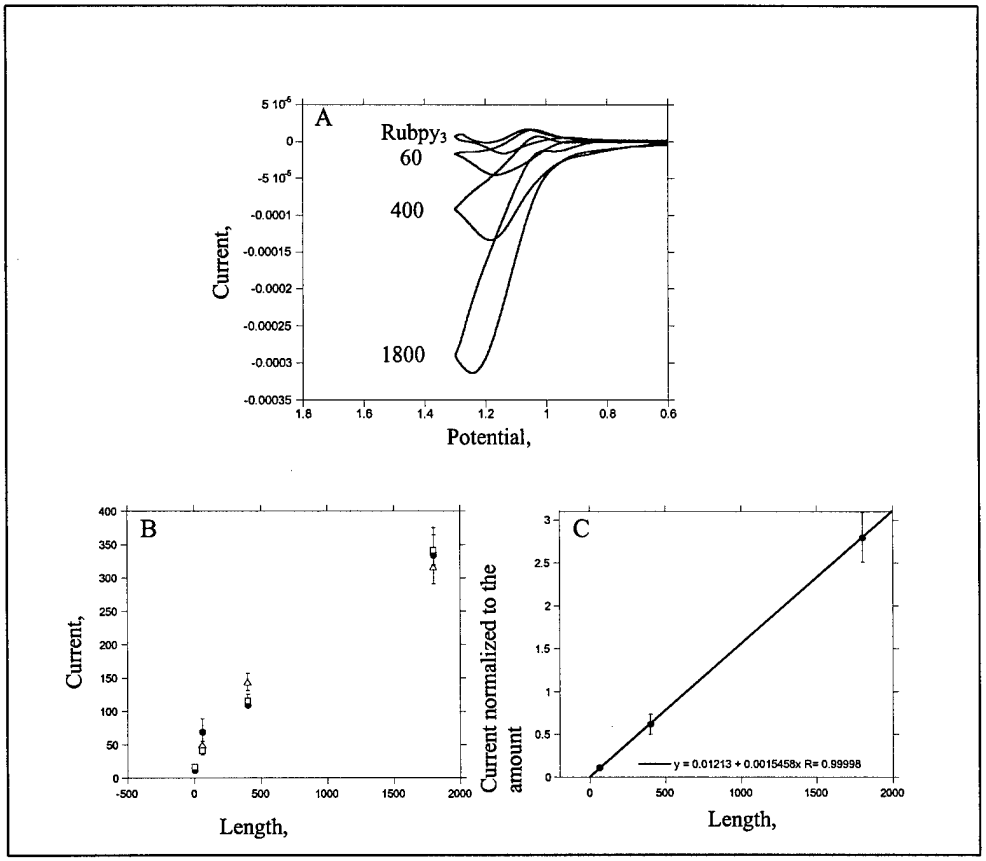

Figure 4. Electrochemical data for $(CGG{\cdot}CCG)_n$ oligonucleotide and PCR products. **(A)** Respresentative set of cyclic voltammograms of DNA-modified ITO electrodes with 25 uM $Ru(bpy)_3^{2+}$ in 50 mM sodium phosphate, pH 7 taken at 10 V/sec. **(B)** Average peak current as a function of DNA length. Each point represents a mean value with one standard deviation of three electrodes. Three sets of symbols represent three individual experiments. **(C)** Peak current from triangles (Δ) in (B) normalized to the amount of DNA immobilized.

Experimental. *Materials.* Synthetic oligonucleotides were purchased from the Nucleic Acid Core Facility at the Lineberger Comprehensive Cancer Center at the University of North Carolina at Chapel Hill and purified on Microcon YM-3 centrifugal filters (Millipore). Water was purified with a MilliQ purification system (Millipore). Reagents for buffer preparation were purchased from Gibco BRL or Mallinckrodt. SeaKem LE agarose was purchased from FMC BioProducts. $[Ru(bpy)_3]Cl_2$ was purchased from Aldrich and purified by recrystallization from methanol. DNTPs were obtained from Pharmacia.

Polymerase Chain Reaction. $(CTG{\cdot}CAG)_n$ PCR products were generated according to a previously published procedure (*8*) with several modifications. Each 50-μL reaction contained the following: 1 μg d[5'-$(CAG)_{20}$] oligonucleotide, 1 μg d[5'-$(CTG)_{20}$] oligonucleotide, 1X PCR buffer containing 20 mM Tris-HCl, pH 8.5, 16 mM $(NH)_4SO_4$, 2.5 mM $MgCl_2$, and 150 μg/mL BSA (New England Biolabs), 6U Klentaq1 polymerase (Ab Peptides), and 0.1 U Cloned Pfu DNA Polymerase (Stratagene). Concentration of dNTPs (dATP, dCTP, dGTP, and dTTP) was either 150 μM or 300 μM each, depending on the size of the desired PCR product. PCR was performed on PCRSprint thermocycler (Hybaid) with the following cycling profile: 1 min at 94°C,

followed by 25-30 cycles of 30 sec at 92°C, 30 sec at 65°C, 1.5-5 min at 75°C, depending on the size of the desired PCR product. The $(CGG{\cdot}CCG)_n$ PCR products were synthesized in a similar fashion, starting with d[5'-$(CGG)_{20}$] and d[5'-$(CCG)_{20}$] oligonucleotides. The dNTP (only dCTP and dGTP) concentration was increased to 600 μM or 1 mM, depending on the size of the desired PCR product. The $MgCl_2$ concentration was increased to 5 mM for the longer product. The cycling profile was similar to that used for the $(CTG{\cdot}CAG)_n$ repeat, with the only difference being the decreased annealing temperature (from 65°C to 50°C). PCR products were purified using the QIAquick PCR purification kit (Qiagen) according to manufacturer's procedure. Following the purification step, the elution buffer was exchanged for 100 mM sodium acetate, pH 6.8.

Gel Electrophoresis. The resulting PCR products were electrophoresed on a 0.9% agarose gel at 100 V for 1-2 hrs. The gel was stained with ethidium bromide (Sigma) and visualized using a CCD camera (Spectroline). The sizes of DNA fragments were estimated by comparison to 1 kb DNA ladder (Gibco BRL). The gel was scanned on an OpticPro 4800P scanner and average sizes of PCR products were estimated by drawing histograms of the gel lanes in the AAB 1D Main software.

DNA Immobilization. The $(CTG{\cdot}CAG)_{10}$ oligonucleotide and the $(CTG{\cdot}CAG)_n$ PCR products were immobilized on tin-doped indium oxide (ITO) electrodes according to a method developed by Armistead and Thorp (*6*). In this method, ITO electrodes were cleaned by 15-minute sonications in 4 g/L Alconox, isopropanol, and MilliQ water twice. A solution containing 2 μL of 0.25 μM DNA (strand concentration) in 100 mM NaOAc/HOAc, pH 6.8 was added to 18 μL dimethylformamide (DMF). The resulting solution was pipetted in the center of the electrode and incubated in a constant humidity chamber for 1 hr. Electrodes were then washed with MilliQ water twice, 1 M NaCl once, and MilliQ water three times (3 minutes each wash), and air-dried. The $(CGG{\cdot}CCG)_{20}$ oligonucleotide and $(CGG{\cdot}CCG)_n$ PCR products were immobilized onto the electrode surface in a similar fashion except that the Alconox step was omitted during electrode cleaning, solution volume was increased to 3 μL DNA with 27 μL DMF, and incubation time was increased to 6 hrs.

Phosphorimagery. ITO electrodes for phosphorimagery were prepared in the same fashion as for voltammetry experiments, except that a portion of the DNA solution was 5'-[^{32}P]-labeled using T4 polynucleotide kinase (Gibco BRL) and 5'-[γ-^{32}P]-dATP (Amersham) (*11*). Unreacted 5'-[γ-^{32}P]-dATP was removed from the labeled oligonucleotide using ProbeQuant G-50 Microcolumns (Amersham) followed by ethanol precipitation. Prior to applying the sample on G-50 microcolumns, sodium acetate was exchanged for the buffer supplied by manufacturer by one 300-μL wash with 3 M sodium acetate, pH 7 followed by two 300-μL water washes. This step is important because components in the supplied buffer (150 mM NaCl, 10 mM Tris-HCl, pH 8, 1 mM EDTA, and 0.15 % Kathon CG/ICP Biocide preservative) decrease the amount of immobilized DNA. Radiolabeled-DNA-modified electrodes were exposed on a phosphorimager screen overnight and scanned using Storm 840 system (Molecular Dynamics). Quantification was performed in ImageQuaNT software (Molecular Dynamics) by performing volume integration of the equal-area squares drawn around electrodes.

Voltammetry. Cyclic voltammograms were collected using an EG&G Princeton Applied Research 273A potentiostat/galvanostat with a single compartment (*12*)

equipped with a tin-doped indium oxide (ITO) working electrode with a geometric area of 0.32 cm^2 (Delta Technologies), Pt-wire auxiliary electrode, and a Ag/AgCl reference electrode (Cypress Systems). Voltammograms of DNA-modified electrodes were taken from 0 to 1.3 V at 10 V/sec in the presence of 25 μM solution of $Ru(bpy)_3^{2+}$ in 50 mM sodium phosphate, pH 7. Voltammograms of buffer alone on clean ITO electrodes without DNA were used for background subtraction.

Research Accomplishments

- Generation of PCR fragments with trinucleotide repeat sequences of CAG and CCG.
- Immobilization of PCR fragments on ITO electrodes with high reproducibility and good linearity based on the quantity of applied DNA.
- Detection of quantity **and** size of PCR products.

Reportable Outcomes

- Findings reported by Ivana Yang at the Era of Hope Meeting in Atlanta, June 2000.
- Immobilization method reported in Analytical Chemistry: Armistead, P. M.; Thorp, H. H. "Modification of Metal Oxides with Nucleic Acids: Detection of Attomole Quantities of Immobilized DNA by Electrocatalysis." *Anal. Chem.* **2000**, in press.
- Kinetics studies of oxidation at the modified electrodes reported in a paper submitted to the Journal of the American Chemical Society: Oxidation Kinetics of Guanine in DNA Molecules Adsorbed to Indium Tin Oxide Electrodes. P. M. Armistead, H. H. Thorp* *J. Am. Chem. Soc.*, submitted 6/00. (Note that P. M. Armistead also received fellowship support from DoD as DAMD17-96-1-6067.)
- Kinetics of fragment size effects in solution reported in a paper submitted to Inorganic Chemistry: Kinetics of Metal-Mediated, One-Electron Oxidation of Guanine in Polymeric DNA and Oligonucleotides Containing Trinucleotide Repeat Sequences. I. V. Yang, H. H. Thorp* *Inorg. Chem.*, submitted 5/00.

Conclusions

The work performed under this grant has provided a convenient method for immobilizing PCR fragments and quantitating these fragments quickly. The detection can be performed in less than 40 min after completion of the PCR amplification and requires only inexpensive tin oxide electrodes and a low-cost potentiostat. Thus, the method will be amenable to development of inexpensive and portable sensors for PCR fragments, and as we have shown elsewhere, these can be from breast cancer genes such as HER-2 and Rak. In the last year, we have shown that the method can also be used to determine the size of PCR fragments, which will allow for detection of genetic abnormalities and provide the same advantages for RFLP analysis, detection of trinucleotide repeat expansion, and other changes that are reflected in the size of DNA fragments. These studies complete Task 2 in the new Statement of Work that has been submitted to Cheryl Lowery. The final tasks in the new Statement of Work center on miniaturization of the assays developed thus far to allow for application to smaller quantities of material as would be available directly from clinical samples without PCR amplification.

References

1. H. H. Thorp, *Trends Biotechnol.* **16**, 117-121 (1998).
2. D. H. Johnston, K. C. Glasgow, H. H. Thorp, *J. Am. Chem. Soc.* **117**, 8933-8938 (1995); D. H. Johnston, T. W. Welch, H. H. Thorp, *Metal Ions Biol. Syst.* **33**, 297-324 (1996); P. A. Ropp, H. H. Thorp, *Chem. Biol.* **6**, 599-605 (1999).
3. D. H. Johnston, H. H. Thorp, *J. Phys. Chem.* **100**, 13837-13843 (1996).
4. M. E. Napier *et al.*, *Bioconjugate Chem.* **8**, 906-913 (1997).
5. M. E. Napier, H. H. Thorp, *Langmuir* **13**, 6342-6344 (1997).
6. P. M. Armistead, H. H. Thorp, *Anal. Chem.*, in press (2000).
7. H. Nawroz, W. Koch, P. Anker, M. Stroun, D. Sidransky, *Nat. Med.* **2**, 1035-1037 (1996).
8. J. M. Ordway, P. J. Detloff, *BioTechniques* **21**, 609-612 (1996).
9. M. Mitas *et al.*, *Nucleic Acids Res.* **23**, 1050-1059 (1995); A. M. Gacy, C. T. McMurray, *Biochemistry* **37**, 9426-9434 (1998).
10. I. V. Yang, H. H. Thorp, *Inorg. Chem.* Submitted (2000).
11. J. Sambrook, E. F. Fritsch, T. Maniatis, *Molecular cloning: a laboratory manual* (Cold Spring Harbor, Plainview, NY, 1989).
12. J. L. Willit, E. F. Bowden, *J. Phys. Chem.* **94**, 8241-8246 (1990).

Appendices

Three copies of the published paper by Armistead and Thorp are attached.

Modification of Indium Tin Oxide Electrodes with Nucleic Acids: Detection of Attomole Quantities of Immobilized DNA by Electrocatalysis

Paul M. Armistead and H. Holden Thorp*

Department of Chemistry and Lineberger Comprehensive Cancer Center, University of North Carolina, Chapel Hill, North Carolina 27599-3290

Indium tin oxide electrodes were modified with DNA, and the guanines in the immobilized nucleic acid were used as a substrate for electrocatalytic oxidation by $Ru(bpy)_3^{3+}$ (bpy = 2,2′-bipyridine). Nucleic acids were deposited onto 12.6-mm^2 electrodes from 9:1 DMF/water mixtures buffered with sodium acetate. The DNA appeared to denature in the presence of DMF, leading to adsorption of single-stranded DNA. The nucleic acid was not removed by vigorous washing or heating the electrodes in water, although incubation in phosphate buffer overnight liberated the adsorbed biomolecule. Acquisition of cyclic voltammograms or chronoamperomograms of $Ru(bpy)_3^{2+}$ at the modified electrodes produced catalytic signals indicative of oxidation of the immobilized guanine by Ru(III). The electrocatalytic current was a linear function of the extent of modification with a slope of 0.5 μA/pmol of adsorbed guanine; integration of the current−time traces gave 2.2 ± 0.4 electrons/guanine molecule. Use of long DNA strands therefore gave steep responses in terms of the quantity of adsorbed DNA strand. For example, electrodes modified with a 1497-bp PCR product from the HER-2 gene produced detectable catalytic currents when as little as 550 amol of strand was adsorbed, giving a sensitivity of 44 amol/mm^2.

Spatial resolution of nucleic acids immobilized on solid surfaces has enabled the parallel detection of nucleic acids in array formats that have been applied to monitoring the presence of infectious organisms, quantitating mRNA expression levels, and sequencing genomic DNA.[1-3] Factors that have made these advancements possible include fluorescence microscopy, methods to label DNA and RNA with fluorophores, and the ability to attach nucleic acids on small, spatially resolved features. Electrochemical techniques are ideally suited to miniaturization and have the potential to simplify nucleic acid analysis by circumventing the need for fluorescent labeling steps and fluorescent microscopy.[4,5] Numerous methods for attaching DNA to electrode materials have been described.[6-12]

Direct electrochemistry of nucleic acids has been achieved through a number of approaches. The electrochemical detection of nucleic acids was first demonstrated by Palecek using reduction of the guanine, cytosine, and adenine bases at mercury electrodes.[13] This original work has been modified and improved to such an extent that the reduction can be used to detect DNA with a sensitivity of roughly 100 pg.[14,15] Wang et al. have focused on the detection of direct oxidation of the guanine and adenine bases adsorbed on carbon electrodes.[8,16-18] The major difficulty with this approach is that water is also oxidized at the potentials needed to oxidize guanine and adenine; however, by combining square wave voltammetry and standard background subtraction, a detection limit estimated to be 15.4 fmol of tRNA has been achieved on a 2.5-mm-diameter carbon paste electrode.[18] Kuhr et al. have also achieved a sensitive detection system based upon catalytic oxidation of the deoxyribose (or ribose) sugar in nucleic acid at a copper microelectrode.[19-21] To detect low concentrations of nucleotides, a 20-μm-diameter copper wire is used as the working electrode, and sinusoidal voltammetry is performed. To date, this system has been used to detect nucleotide concentrations of 70−200 nM and DNA concentrations of 3.2 pM.[20,21]

(1) Spargo, C. A.; Haaland, P. D.; Jurgensen, S. R.; Shank, D. D.; Walker, G. T. *Mol. Cell. Probes* **1993**, *7*, 395−404.
(2) Schena, M.; Shalon, D.; Davis, R. W.; Brown, P. O. *Science* **1995**, *270*, 467−470.
(3) Chee, M.; Yang, R.; Hubbell, E.; Berno, A.; Huang, X. C.; Stern, D.; Winkler, J.; Lockhart, D. J.; Morris, M. S.; Fodor, S. P. A. *Science* **1996**, *274*, 610−614.
(4) Thorp, H. H. *Trends Biotechnol.* **1998**, *16*, 117−121.
(5) Mikkelsen, S. R. *Electroanalysis* **1996**, *8*, 15−19.
(6) Millan, K. M.; Spurmanis, A. J.; Mikkelsen, S. R. *Electroanalysis* **1992**, *4*, 929−932.
(7) Palecek, E. *Electroanalysis* **1996**, *8*, 7−14.
(8) Wang, J.; Cai, X.; Rivas, G.; Shiraishi, H.; Farias, P. A. M.; Dontha, N. *Anal. Chem.* **1996**, *68*, 2629−2634.
(9) Kourl-Yousoufi, H.; Garnier, F.; Srivasta, P.; Yassar, A. *J. Am. Chem. soc.* **1997**, *119*, 7388−7389.
(10) Herne, T. M.; Tarlov, M. J. *J. Am. Chem. Soc.* **1997**, *119*, 8916−8920.
(11) de Lumley-Woodyear, T.; Caruana, D. J.; Campbell, C. N.; Heller, A. *Anal. Chem.* **1999**, *71*, 394−398.
(12) de Lumley-Woodyear, T.; Campbell, C. N.; Freeman, E.; Freeman, A.; Georgiou, G.; Heller, A. *Anal. Chem.* **1999**, *71*, 535−538.
(13) Palecek, E. *Nature* **1960**, *188*, 656−657.
(14) Palecek, E.; Fojta, M. *Anal. Chem.* **1994**, *66*, 1566−1571.
(15) Palecek, E.; Tomschik, M.; Stankova, V.; Havran, L. *Electroanalysis* **1997**, *9*, 990−997.
(16) Wang, J.; Cai, X.; Jonsson, C.; Balakrishnan, M. *Electroanalysis* **1996**, *8*, 20−24.
(17) Wang, J.; Fernandes, J. R.; Kubota, L. T. *Anal. Chem.* **1998**, *70*, 3699−3702.
(18) Wang, J.; Bollo, S.; Paz, J. L. L.; Sahlin, E.; Mukherjee, B. *Anal. Chem.* **1999**, *71*, 1919−1931.
(19) Singhal, P.; Kawagoe, K. T.; Christian, C. N.; Kuhr, W. G. *Anal. Chem.* **1997**, *69*, 1662−1668.
(20) Singhal, P.; Kuhr, W. G. *Anal. Chem.* **1997**, *69*, 3552−3557.
(21) Singhal, P.; Kuhr, W. G. *Anal. Chem.* **1997**, *69*, 4828−4832.

10.1021/ac000051e CCC: $19.00
Published on Web 00/00/0000

The poor electron-transfer kinetics from nucleic acids to most electrode materials has led many research groups to investigate the utility of having the detection of nucleic acids coupled to the detection of some second reporter molecule. Mikkelsen and coworkers detected DNA on carbon electrodes by immobilizing the DNA onto the electrode and then measuring the enhanced faradaic current of $Co(bpy)_3^{2+/3+}$ in the presence of the surface-attached DNA; the detection limit of this system was estimated to be 250 pg of a 400-bp PCR product.[22,23] Another indirect detection system recently reported by Heller et al. involves the modification of DNA to allow coupling to a "wired" polymer on the electrode surface.[12] A genetically modified horseradish peroxidase is added to the DNA-treated polymer, and in the presence of hydrogen peroxide substrate, Heller et al. detected a modified PCR product in 10 min and a single base mismatch in an oligonucleotide on a 7-μm microelectrode.[12,24] Another recent indirect system involves monitoring the redox chemistry of methylene blue on alkanethiol monolayers of DNA on gold electrodes.[25,26]

An approach taken by our laboratory to address the issue of creating a sensitive nucleic acid detection system involves using $Ru(bpy)_3^{2+/3+}$ as a guanine oxidation catalyst (bpy = 2,2′-bipyridine).[4,27] Using $Ru(bpy)_3^{2+}$ as the oxidation catalyst for guanine offers an advantage over detecting guanine oxidation directly because it exhibits rapid electron-transfer kinetics with most electrode materials including the tin-doped indium oxide (ITO) electrodes used in this study.[28] $Ru(bpy)_3^{3+}$ has a reduction potential of 1.06 V vs Ag/AgCl, which is close to that of guanosine radical cation (E° = 1.07 V vs Ag/AgCl);[29] second-order rate constants for electron transfer from guanine in DNA to $Ru(bpy)_3^{3+}$ are as high as 10^6 M^{-1} s^{-1}.[30-33] The $Ru(bpy)_3^{3+}$–guanine electron transfer is observed as a current enhancement in the oxidation wave of $Ru(bpy)_3^{2+}$ in a cyclic voltammogram through an EC′ mechanism:[34-36]

$$Ru(bpy)_3^{2+} \rightarrow Ru(bpy)_3^{3+} + e^- \quad (1)$$

$$Ru(bpy)_3^{3+} + \text{guanine} \rightarrow Ru(bpy)_3^{2+} + (\text{guanine})^+ \quad (2)$$

The ITO electrodes exhibit little water oxidation current at the potentials needed to achieve the electrocatalysis.[28]

To make this reaction scheme practical for use as a nucleic acid biosensor, surface immobilization of the nucleic acid must be achieved.[4] We have pursued a number of immobilization schemes involving self-assembled monolayers,[35] electropolymerized films,[37] and porous membranes attached to the ITO surface.[36] Here we describe a very simple system for immobilizing DNA on ITO without the use of a coupling agent or an additional layer on the electrode. In this approach, strands of DNA 435–1497 bp long were prepared by polymerase chain reaction (PCR) and directly attached to an ITO surface by irreversible adsorption of the DNA from a *N,N*-dimethylformamide (DMF)/acetate solution. Repeated washing or heating of the electrodes did not liberate the immobilized DNA. Guanines in the immobilized DNA did not show significant direct oxidation current, but did act as a substrate for the electrocatalysis scheme shown in eqs 1 and 2 with $Ru(bpy)_3^{2+}$ in solution. Quantification of the adsorbed DNA by radiolabeling and phosphorimagery showed that less than 1 fmol of long strands of DNA gave measurable catalytic currents on relatively large electrodes (12.6 mm^2), giving a detection limit of only 44 amol/mm^2. The fragments detected were RT-PCR amplicons of the HER-2 mRNA from BT-474 cancer cells. Amplification of the HER-2 gene correlates with decreased survival in women with node-positive breast cancer.[38]

EXPERIMENTAL SECTION

Preparation of Nucleic Acids. BT-474 cells were kindly provided by the laboratory of Dr. Bill Cance at the UNC Lineberger Comprehensive Cancer Center. RNA was extracted and purified by means of an RNeasy RNA purification kit from Qiagen. Polymerase chain reaction was performed using a Hybaid PCR Sprint with a 0.2-mL tube configuration heating block. PCR products were purified on Life Technologies Concert PCR purification columns (Life Technologies). Quantification of radiolabeled PCR products was performed on a Molecular Dynamics Storm 860 phosphorimager with subsequent analysis performed using ImageQuaNT software. All water used was in-house distilled water that was further purified through a Milli-Q ultrafiltration system. Water used for RNA manipulations was further treated with diethyl pyrocarbonate (DEPC; Sigma).

Reverse transcription was performed by mixing 2 μL of total RNA (0.8 μg/μL), 2 μL of Random hexamers (Promega), 4 μL of dNTPs (10 mM, Amersham), and 6 μL of RNase-free water. The reverse transcription mix was heated to 70 °C for 3 min to denature the RNA and then immediately placed on ice. To the mix was added 1 μL of RNasin (Promega), 1 μL of M-MLV reverse transcriptase (Life Technologies, 200 units/μL), and 4 μL of 5× reverse transcription buffer (Life Technologies). The reactants were mixed and incubated at 42 °C for 1 h. PCR was performed on the reverse transcription products to amplify segments of the HER-2 gene. A 50-μL PCR mix was assembled from 5 μL of the reverse transcription reaction, 2.5 μL of the forward primer (5 μM), 2.5 μL of the reverse primer (5 μM), 2.5 μL of $MgCl_2$ (50 mM), 2.5 μL of dNTPs (10 mM), 5 μL of 10× PCR buffer, 30 μL of water, and 1 unit of Taq polymerase (Life Technologies, 5 units/μL). The 435-bp product (forward primer, GGC TGT GCC

(22) Millan, K. M.; Mikkelsen, S. R. *Anal. Chem.* **1993**, *65*, 2317–2323.
(23) Millan, K. M.; Saraulio, A.; Mikkelsen, S. R. *Anal. Chem.* **1994**, *66*, 2943–2948.
(24) Carauna, D. J.; Heller, A. *J. Am. Chem. Soc.* **1999**, *121*, 769–774.
(25) Kelley, S. O.; Boon, E. M.; Barton, J. K.; Jackson, N. M.; Hill, M. G. *Nucleic Acids Res.* **1999**, *27*, 4830–4837.
(26) Kelley, S. O.; Barton, J. K.; Jackson, N. M.; Hill, M. G. *Bioconjugate Chem.* **1997**, *8*, 31–37.
(27) Johnston, D. H.; Welch, T. W.; Thorp, H. H. *Metal Ions Biol. Syst.* **1996**, *33*, 297–324.
(28) Johnston, D. H.; Glasgow, K. C.; Thorp, H. H. *J. Am. Chem. Soc.* **1995**, *117*, 8933–8938.
(29) Steenken, S.; Jovanovic, S. V. *J. Am. Chem. Soc.* **1997**, *119*, 617–618.
(30) Sistare, M. F.; Holmberg, R. C.; Thorp, H. H. *J. Phys. Chem. B* **1999**, *103*, 10718–10728.
(31) Johnston, D. H.; Thorp, H. H. *J. Phys. Chem.* **1996**, *100*, 13837–13843.
(32) Szalai, V. A.; Thorp, H. H. *J. Am. Chem. Soc.* **2000**, *122*, 4524–4525.
(33) Ropp, P. A.; Thorp, H. H. *Chem. Biol.* **1999**, *6*, 599–605.
(34) Napier, M. E.; Loomis, C. R.; Sistare, M. F.; Kim, J.; Eckhardt, A. E.; Thorp, H. H. *Bioconjugate Chem.* **1997**, *8*, 906–913.
(35) Napier, M. E.; Thorp, H. H. *Langmuir* **1997**, *13*, 6342–6344.
(36) Napier, M. E.; Thorp, H. H. *J. Fluoresc.* **1999**, *9*, 181–186.
(37) Ontko, A. C.; Armistead, P. M.; Kircus, S. R.; Thorp, H. H. *Inorg. Chem.* **1999**, *38*, 1842–1846.
(38) Slamon, D. J.; Clark, G. M.; Wong, S. G.; Levin, W. J.; Ullrich, A.; McGuire, W. L. *Science* **1987**, *235*, 177–182.

CGC TGC AAG GGG CCA; reverse primer, GCA GCC AGC AAA CTC CTG GAT ATT), 1,020 bp product (forward primer, GGC TGT GCC CGC TGC AAG GGG CCA; reverse primer, CGG CAA ACAGTG CCT GGC ATT) and 1497-bp PCR product (forward primer, GGC TGT GCC CGC TGC AAG GGG CCA; reverse primer, CCT CAG CTCCGT CTCTTT CAG) were prepared using 1 cycle at 95 °C for 5 min, 30 cycles at 94 °C for 20 s, 62 °C for 30 s (64 °C for the 1020-bp fragment and 55 °C for the 435-bp fragment), 72 °C for 2 min (1.5 min for the 1020-bp fragment and 40 s for the 435-bp fragment), and 1 cycle at 72 °C for 10 min (5 min for the 435-bp fragment). Each PCR product was tested for purity by gel electrophoresis on a 2% agarose gel. Both the 435- and 1497-bp sequences yielded one product of the appropriate size as determined on the gel. The 1020-bp sequence consistently yielded a low molecular weight band that was less than 1% as intense as the major band of the appropriate size observed on the gel. RT-PCR products were purified on Concert purification columns (Life Technologies) before subsequent manipulations. These products were used as templates for further amplifications as more product was needed. The purified PCR products were ethanol precipitated and resuspended in 100 mM sodium acetate at pH 6.8. This procedure typically yielded ~70 μL of 1 mM PCR product (concentration determined in moles of nucleotide) from 20 reaction tubes. Only purified PCR products were used in all of these experiments because the pyrophosphate and unreacted dNTPs in the unpurified PCR mixture adsorb to the electrode. The adsorption of these small molecules prevents adsorption of the DNA product and results in no catalytic current enhancement when electrochemical measurements are performed.

Electrode Modification. ITO electrodes (12.6 mm^2) were purchased from Delta Technologies. ITO electrodes were sonicated in an Alconox (Alconox, New York, NY) solution (8 g of Alconox/L of water) for 15 min, rinsed, and then sonicated in 2-propanol for 15 min followed by two 15-min sonications in water.[39] The electrodes were then allowed to air-dry. Purified PCR products were prepared for immobilization onto the ITO surface by mixing 5 μL of the PCR product in 100 mM sodium acetate, pH 6.8, with 45 μL of DMF. The 50-μL mixture was pipetted onto each electrode, and the electrodes were placed in a constant-humidity chamber for 1 h. The electrodes were then rinsed by immersion in solutions that were agitated on a rotary mixer. The electrodes were subjected to two water washes for 3 min each, one wash in 1 M sodium chloride for 5 min, one wash in 100 mM sodium phosphate (pH 7.0) for 5 min, and three final washes in water each for 3 min. The electrodes were then allowed to dry. The amount of DNA attached to the surface was controlled by changing the concentration of the PCR product that was applied to the ITO.

Electrochemical Measurements. All electrochemical experiments were performed in a one-compartment electrochemical cell using a BAS 100B potentiostat. The modified ITO was used as the working electrode, a Ag/AgCl (Cypress Systems) minielectrode was used as the reference, and a platinum wire was used as the auxiliary electrode. For each batch of 10 electrodes cleaned, one electrode was used to perform a background scan. This electrode was not treated with DNA; however, cyclic voltammetry was performed on it at the above parameters without $Ru(bpy)_3^{2+}$ in 50 mM sodium phosphate, pH 7.0. This buffer cyclic voltammogram was subtracted from those later measured on the DNA-modified electrodes. As measurements at lower DNA concentrations were performed, the effect of background-subtraction error increased. Background-subtracted cyclic voltammograms whose charging current contribution was greater than the actual faradaic signal of $Ru(bpy)_3^{2+}$ oxidation were not used in subsequent analyses.

DNA Quantification by Phosphorimagery. Radiolabeled PCR products were synthesized according to a method similar to that of Mertz and Rashtchian.[40] Briefly, a 20-μL PCR mixture was prepared containing 1 μL of template DNA (100 pg/μL), 1 μL of forward primer (5 μM), 1 μL of reverse primer (1 μL of $MgCl_2$ (10 mM), 1 μL of dNTP's (100 μM), 2 μL of 10× PCR buffer, 3 μL of α-^{32}P-dCTP (1.8 μM), 10 μL of water, and 1 unit of Taq polymerase. Preparation of the appropriate fragment was verified by electrophoresis of parallel, nonradioactive PCR products on a 5% native polyacrylamide gel stained with SYBR-green (Molecular Probes). All of the parallel reactions yielded one visible product that was the appropriate length. The radiolabeled PCR products were purified on Concert PCR purification cartridges, ethanol precipitated, and dried on a speed vacuum. To each dried radiolabeled PCR product was added 40 μL of 1 mM unlabeled PCR product of the same length in 100 mM sodium acetate, pH 6.8. The newly doped PCR products were used within 1 day of synthesis to minimize the effects of radiolysis. Electrodes modified with radiolabeled DNA were air-dried, wrapped in plastic wrap, and placed on a phosphorimager screen. Aliquots of 1 μL of certain concentrations from the labeled PCR products were used as quantification standards. These aliquots were applied to filter paper, dried, wrapped in plastic wrap, and placed on the phosphorimager screen. The phosphorimager screen was exposed for ~12 h and scanned on a Molecular Dynamics Storm 860 phosphorimager.

RESULTS

Electrocatalysis at DNA-Modified Electrodes. To maximize the sensitivity of the electrocatalytic system, conditions were established to minimize current due to $Ru(bpy)_3^{2+}$ alone and to maximize the contribution of the catalytic signal. The ratio of the catalytic current (i_{cat}) to current at the unmodified electrode (i_d) was determined as a function of scan rate and $Ru(bpy)_3^{2+}$ concentration. The maximum value of i_{cat}/i_d was observed when voltammograms were collected at a scan rate of 10 V/s, and the $Ru(bpy)_3^{2+}$ concentration was kept at only 10 μM. At lower scan rates or higher concentrations of $Ru(bpy)_3^{2+}$, the catalytic current was more difficult to distinguish over the current due to the metal complex alone. Shown in Figure 1A are cyclic voltammograms of $Ru(bpy)_3^{2+}$ at a DNA-modified electrode (solid line) and of an unmodified electrode over the same potential range in 50 mM phosphate buffer with no $Ru(bpy)_3^{2+}$ (dashed line). The DNA-modified electrode gave faradaic currents that were large in the forward direction current and small in the reverse direction, as is typical of electrocatalysis. This faradaic wave was superimposed on a relatively high charging current that results from the large electrode area (12.6 mm^2) and the high scan rate.

Figure 1B shows background-subtracted voltammograms of $Ru(bpy)_3^{2+}$ at DNA-modified (solid line) and unmodified (dashed

(39) Willit, J. L.; Bowden, E. F. *J. Phys. Chem.* **1990**, *94*, 8241–8246.

(40) Mertz, L. M.; Rashtchian, A. *Focus* **1994**, *16*, 45–48.

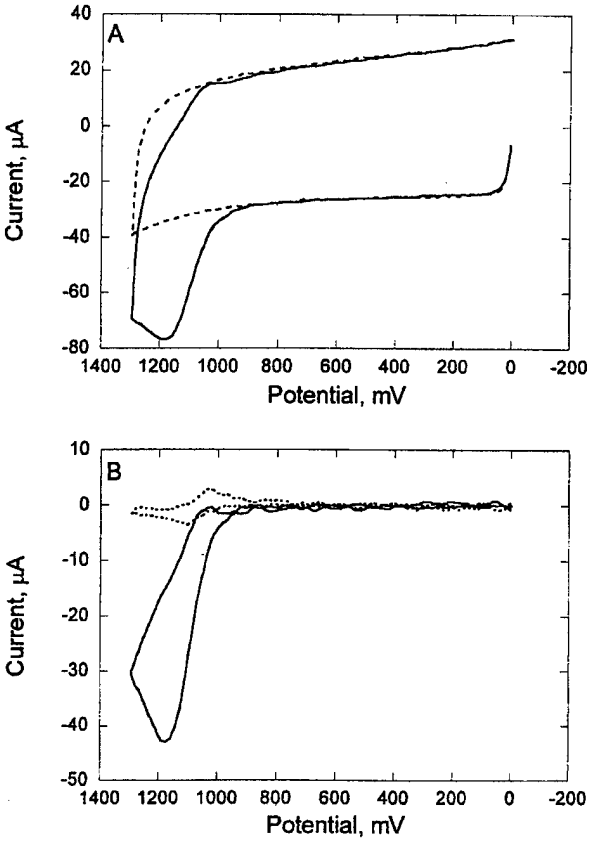

Figure 1. (A) Cyclic voltammograms taken at 10 V/s for bare ITO in 50 mM sodium phosphate, pH 7 (dashed line) and for a DNA-modified electrode in 10 μM $Ru(bpy)_3^{2+}$ (solid line). (B) Cyclic voltammograms obtained after subtraction for 10 μM $Ru(bpy)_3^{2+}$ at an unmodified electrode (dashed line) and at the DNA-modified electrode from (A) (solid line). Subtractions used as a background scan of bare ITO in 50 mM sodium phosphate, as shown as the dashed line in (A).

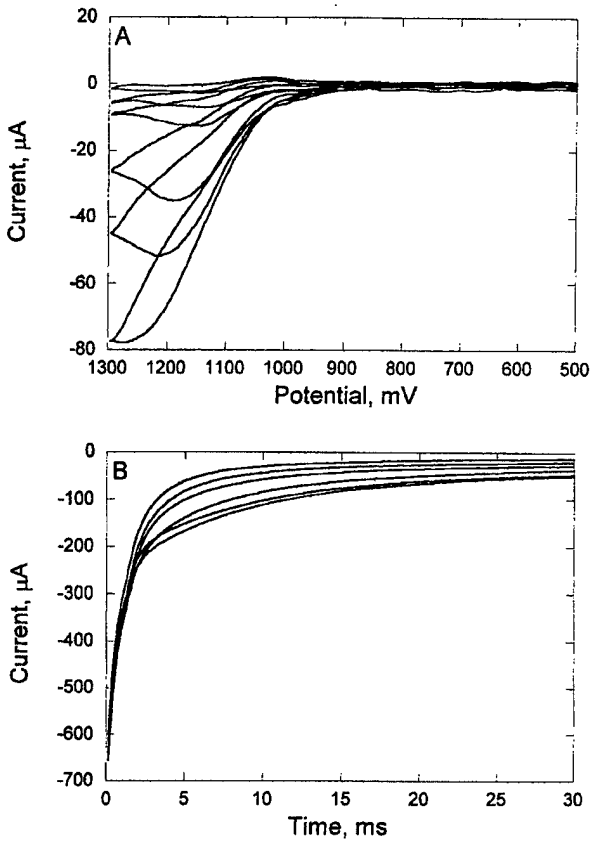

Figure 2. (A) Cyclic voltammograms of 10 μM $Ru(bpy)_3^{2+}$ at ITO electrodes modified with 1497-bp PCR product at nucleotide concentrations of 50, 20, 10, 2.5, 1.0, and 0.5 μM. Increasingly larger currents were observed as the DNA concentration increased. (B) Representative chronoamperograms of 10 μM $Ru(bpy)_3^{2+}$ at ITO electrodes modified with the 435-bp PCR product at the same nucleotide concentrations as in (A).

line) electrodes. The catalytic enhancement due to the immobilized DNA is apparent in comparing the two voltammograms. The voltammogram at the unmodified electrode shows the typical quasi-reversible response for $Ru(bpy)_3^{2+}$ at these scan rates and gives an oxidative peak current of 3.6 ± 0.6 μA over more than 20 trials. Voltammograms of the DNA-modified electrodes in the *absence* of $Ru(bpy)_3^{2+}$ produced a barely detectable current above that observed for the unmodified electrodes; i.e., very little oxidation of guanine in the immobilized DNA was detected without $Ru(bpy)_3^{2+}$. Further, repeated scanning of the electrodes modified with 100 μM DNA in the presence of $Ru(bpy)_3^{2+}$ produced much smaller currents on the second scan, and by the tenth scan, the signal had decreased to 4.1 μA, within experimental error of the value for $Ru(bpy)_3^{2+}$ at an unmodified electrode. This result suggests that the electrocatalysis irreversibly damages the guanine bases in the DNA.

The DNA-modified electrode in Figure 1 was prepared by treating an ITO electrode with a 20 μM (nucleotide) solution of DNA in 9:1 DMF/acetate buffer at constant humidity for 1 h followed by numerous washing steps that did not remove the immobilized DNA. No DNA was lost even after heating the electrodes to 95 °C for 2 min; however, the DNA could be removed by incubation in phosphate buffer at room temperature overnight. This competition by phosphate did cause removal of up to 50% of the immobilized DNA during the sodium phosphate rinsing step; however, provided the washing time was carefully followed, reproducible results were obtained. Figure 2A shows representative cyclic voltammetry data obtained from electrodes modified with increasingly concentrated solutions of DNA. As the quantity of DNA exposed to the electrode was increased, the catalytic current increased both in cyclic voltammetry (Figure 2A) and in chronoamperometry (Figure 2B). Note that the voltammograms in Figure 2A were performed with electrodes modified with the larger PCR product while the chronoamperometry data were collected on electrodes modified with the shorter fragment and thus were modified with less total guanine (vide infra). Nevertheless, increases in current attributable to DNA oxidation were generally more readily apparent in the raw data obtained by cyclic voltammetry than by chronoamperometry.

An important question was whether the immobilized DNA was in the single-stranded or duplex form. In the experiments thus far, double-stranded PCR products were added to the DMF solution that was then placed on the ITO electrode for immobilization. We suspected that the DMF solution denatured the duplexes, leading to immobilization of single-stranded DNA. Cyclic voltam-

Table 1. Immobilization of PCR Products on ITO Electrodes

strand length (bp)	nucleotide concn[a] (μM)	strand concn[b] (nM)	nucleotide immobilized[c] (pmol)	strand immobilized[d] (fmol)	% immobilized[e]	peak current[f] (μA)
435	20	23.0	7.7	8.9	14	22.0 ± 4.0
	2	2.30	0.89	1.0	16	3.8 ± 0.5
1020	20	9.80	15	7.4	27	27.0 ± 5.0
	2	0.980	1.4	0.69	25	5.2 ± 0.5
1497	20	6.7	19	6.1	33	38.0 ± 3.0
	2	0.67	1.7	0.55	29	7.1 ± 1.4

[a] Concentration is nucleotide phosphates in the 9:1 DMF/acetate solution applied to the electrode. [b] Strand concentration determined dividing the nucleotide concentration by twice the strand length. [c] Nucleotide immobilized determined by phosphorimagery of ITO electrodes compared to standards of known molar amounts. [d] Strand immobilized determined by dividing the moles of immobilized nucleotide by twice the strand length. [e] Percent immobilized determined by dividing the moles of nucleotide immobilized by the moles of nucleotide applied to the electrode. [f] Oxidative peak current determined for four cyclic voltammograms of $Ru(bpy)_3^{2+}$ at electrodes modified with the given strand concentration; peak current for $Ru(bpy)_3^{2+}$ at an unmodified electrode was 3.6 ± 0.6 μA.

mograms of electrodes with calf thymus DNA that was thermally denatured before the addition of DMF were indistinguishable from cyclic voltammograms obtained from electrodes that were treated with double-stranded DNA. Since calf thymus DNA does not reanneal upon cooling after thermal denaturation, this result strongly suggests that the immobilized DNA is single-stranded.

Characterization of DNA Adsorption. To confirm that DNA was irreversibly adsorbing to the ITO electrodes and that the quantity of adsorbed DNA was increasing as the concentration of the modifying solution was increased, DNA fragments were radiolabeled and quantified using a phosphorimager. The fragments were "body labeled" by performing PCR with α-^{32}P-dCTP, which inserts many radioactive phosphorus nuclei per DNA fragment. The body-labeling scheme was used so that the majority of DNA attached to the electrode could be unlabeled and doped with small quantities of the radiolabeled DNA that had a high specific activity. After the radioactive DNA fragments were attached, the electrodes were placed on a phosphorimager screen and analyzed against standards of known quantity. To determine whether the length of the DNA strands impacted the extent of modification of the electrode, PCR fragments of 435, 1020, and 1497 bp were prepared and used to modify the ITO electrodes. The relevant quantities that need to be considered in the analysis are the nucleotide concentration in the solution, the strand concentration in solution, the quantity of nucleotides immobilized, and the quantity of strands immobilized. Since the immobilized DNA is single-stranded, the number of strands immobilized on the electrode is equal to the quantity of nucleotides on the electrode divided by twice the length of the (double-stranded) PCR product.

The quantities of immobilized strands and nucleotides are compared in Figure 3 and Table 1. For all three PCR products, the number of strands immobilized increases rapidly with the concentration of nucleotides in the application solution until ~40 μM nucleotide, where the fraction of adsorbed DNA begins to decrease (Figure 3A). As a control, the procedure was repeated with borosilicate glass, and the quantity of adsorbed DNA was at least 50 times lower than that adsorbed to ITO. The number of strands immobilized is higher for a given nucleotide concentration for the shorter strands, as also shown in Figure 3A. This effect arises in part because, at a particular nucleotide concentration, a solution of shorter fragments contains a higher number of strands. In fact, when the number of strands immobilized onto the

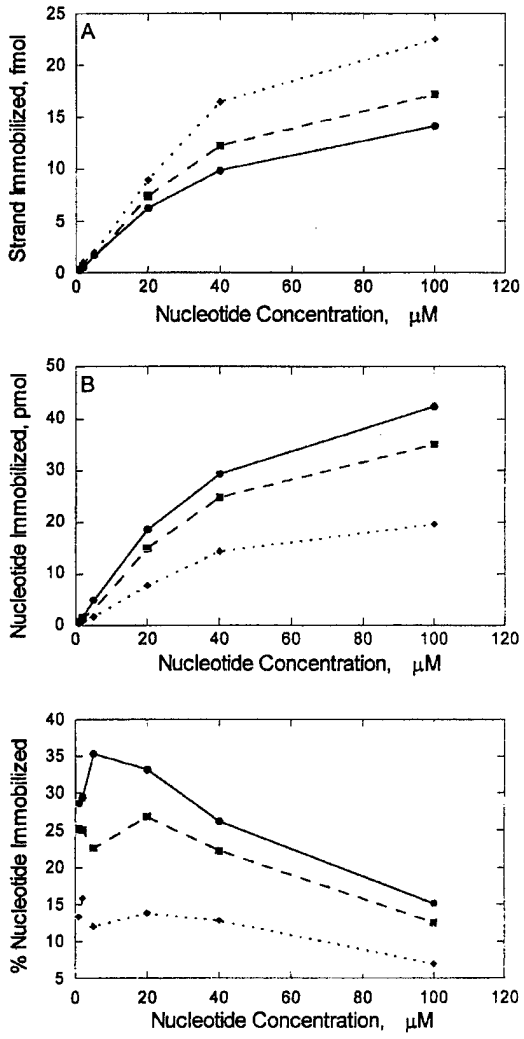

Figure 3. (A) Moles of radiolabeled PCR products immobilized onto ITO electrodes for the PCR products of 1497 (●), 1020 (■), or 435 bp (◆) as a function of the concentration of nucleotide originally applied to the electrode. (B) Moles nucleotides immobilized taken directly from the data in (A). (C) Fraction of nucleotides adsorbed from the deposition solution as a function of the original concentration of the applied solution for the three PCR products.

electrode is converted to the number of nucleotides immobilized (Figure 3B), it is apparent that more total nucleotides are immobilized for the longer fragments. This relationship is also seen in Table 1 by comparing, for example, the results for application of 20 μM nucleotide of the 435-bp fragment, which leads to 7.7 pmol of immobilized nucleotide, while application of 20 μM of the 1497-bp fragment leads to immobilization of 19 pmol of nucleotide. Thus, more than twice the number of nucleotides are immobilized for the longer fragment from solutions containing the same number of nucleotides for each fragment.

The results in Figure 3A and B show that the mechanism of DNA adsorption is one in which generally longer strands lead to a higher efficiency of surface modification at any given nucleotide concentration. Thus, we expect that, for a given concentration of nucleotides, a greater fraction of the total DNA in the solution will be adsorbed with longer strands. We therefore analyzed the number of nucleotides that were adsorbed to the electrode compared to the total number of nucleotides in the solution used to treat the electrode. As expected, a greater fraction of the nucleotides was adsorbed for the longer strands (Figure 3C, Table 1). As much as 33% of the total nucleotides applied to the electrode could be immobilized for the longest strand. In addition, it was apparent for the long strand that the efficiency of modification increases at low nucleotide concentrations and then decreases at higher nucleotide concentrations, as shown in Figure 3C.

The results to this point demonstrate that when more DNA is applied to the electrode, greater catalytic enhancement is obtained for the cyclic voltammetry and chronoamperometry of $Ru(bpy)_3^{2+}$. The independent quantification of the immobilized DNA by phosphorimagery shows that more nucleotides are in fact adsorbed to the electrode at the higher concentrations, and we know from numerous previous studies that the guanines in DNA are the ultimate source of the electrons.[34-37,41]

Sensitivity of Electrocatalytic Detection. We next sought to establish a quantitative relationship between the number of strands adsorbed and the peak current obtained in cyclic voltammograms acquired as in Figure 1. The three fragments chosen all contain ~30% guanine: the 435-bp fragment contains 264 guanines (30.3%), the 1020-bp fragment contains 626 guanines (30.7%), and the 1497-bp fragment contains 918 guanines (30.7%).[42] We therefore expect a direct relationship between the quantity of immobilized nucleotides and the catalytic enhancement, which should be the same for all three sequences. We prepared electrodes modified with all three strands, collected cyclic voltammograms of $Ru(bpy)_3^{2+}$ at each modified electrode, and independently quantified the number of immobilized strands by phosphorimagery. Figure 4A shows there is an excellent linear correlation between the peak current and the number of nucleotides immobilized. The slope of the linear fit is 1.7 μA/pmol nucleotide immobilized, which corresponds to 0.5 μA/pmol guanine. Integrating the peak currents reveals that 2.2 $\pm$ 0.4 electrons are transferred per guanine. There are a number of oxidation pathways for guanine that can result in a two-electron oxidation.[43-47] Representative peak currents are also shown in Table 1 with standard errors.

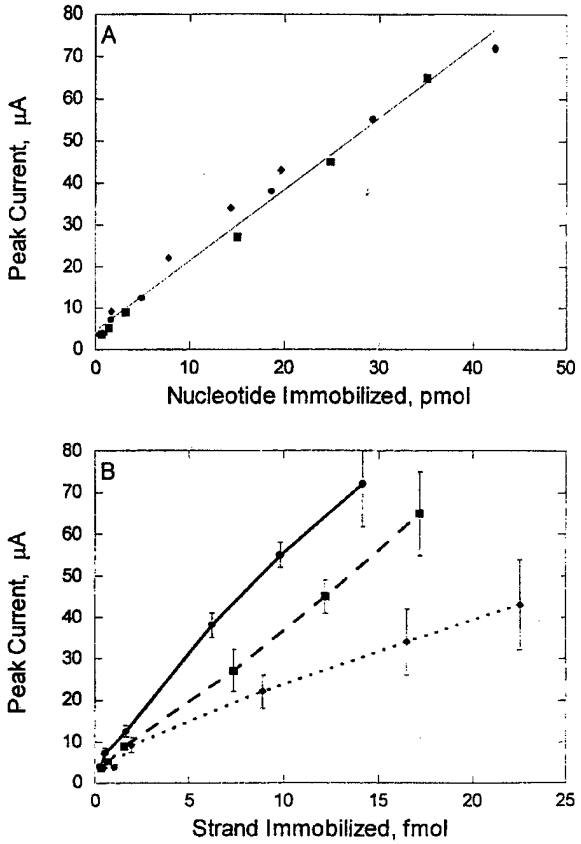

Figure 4. (A) Oxidative peak currents from cyclic voltammograms of 10 μM $Ru(bpy)_3^{2+}$ at the modified electrodes as a function of the quantity of immobilized nucleotides (1497- (●), 1020- (■), and 435-bp PCR product (◆)) determined by phosphorimagery of the radiolabeled PCR products. Voltammograms were acquired as in Figures 1 and 2A. (B) Peak current as a function of moles of strand immobilized for the 1497- (●), 1020- (■), and 435-bp PCR product (◆).

A final prediction that can be made from the results thus far is that the sensitivity of the electrocatalysis to the number of immobilized strands should be steeper for longer fragments that contain more guanines. The data from Figure 4A are replotted in Figure 4B for each fragment as a function of the number of immobilized strands. As expected, the longer fragments show steeper responses. To assess the lower detection limit, the standard error was determined for $Ru(bpy)_3^{2+}$ at unmodified electrodes over numerous trials. Catalytic currents that were more than 3 times greater than this error were detected for the long strand when as little as 550 amol was adsorbed. Thus, the electrocatalysis provides detectable currents at a density of immobilized DNA of 44 amol/mm^2. Even longer DNA fragments

(41) Johnston, D. H.; Cheng, C.-C.; Campbell, K. J.; Thorp, H. H. *Inorg. Chem.* **1994**, *33*, 6388–6390.
(42) Yamamoto, T.; Ikawa, S.; Akiyama, T.; Semba, K.; Nomura, N.; Miyajima, N.; Saito, T.; Toyoshima, K. *Nature* **1986**, *319*, 230–234.
(43) Duarte, V.; Muller, J. G.; Burrows, C. J. *Nucleic Acids Res.* **1999**, *27*, 496–502.
(44) Doddridge, Z. A.; Cullis, P. M.; Jones, G. D. D.; Malone, M. E. *J. Am. Chem. Soc.* **1998**, *120*, 10998–10999.
(45) Cullis, P. M.; Malone, M. E.; Merson-Davies, L. A. *J. Am. Chem. Soc.* **1996**, *118*, 2775–2781.
(46) Vialas, C.; Pratviel, G.; Claparols, C.; Meunier, B. *J. Am. Chem. Soc.* **1998**, *120*, 11548–11553.
(47) Vialas, C.; Claparols, C.; Pratviel, G.; Meunier, B. *J. Am. Chem. Soc.* **2000**, *122*, 2157–2167.

would contain more guanines and give higher signals per strand; however, most reverse transcriptase enzymes cannot reverse transcribe through RNA that has regions containing a high degree of secondary structure, thereby prohibiting production of significantly longer fragments.[48]

DISCUSSION

DNA–Electrode Interaction. When DNA is dissolved in aqueous solution, relatively little adsorption to ITO electrodes is observed. In fact, the direct oxidation of DNA at ITO is difficult to detect in contrast to other electrode materials such as carbon paste and mercury, which give strong DNA adsorption and faradaic current due to base redox chemistry.[15,18] However, when DNA is dissolved in a medium that contains mostly DMF, strong adsorption occurs to produce modified electrodes where the DNA cannot be removed by agitated washing or heating to 95 °C. Given that DNA immobilized in this fashion is slowly released in the presence of phosphate buffer and that longer strands adsorb more efficiently than shorter strands (on a per nucleotide basis), we suspect that a metal–phosphate interaction is partly responsible for the surface modification. Such a model would also explain why borosilicate did not adsorb DNA under the same conditions. Phosphates and phosphonates exhibit high-affinity interactions with metal oxides,[49–51] and it seems reasonable to propose that DNA can form strong associations with ITO through multiple interactions with the phosphate backbone. The fact that DNA remains attached to the surface at high temperatures but can be competed away from the surface by small molecules is a characteristic of polyelectrolyte adsorption.[52]

The extent of surface coverage in these experiments can be assessed from the quantities of adsorbed DNA. With the large fragment, the maximum amount of DNA adsorbed was 14 fmol of duplex. Since the DNA appears to be single-stranded, this translates to 28 fmol of single strands or 1.3×10^9 strands/mm^2. Estimating the footprint of a 1497-base strand as 10 Å × 3.4 Å × 1497 suggests that this quantity of strands covers 8.7 mm^2 or 69% of a full monolayer.[53] The lower limit of detection observed at 550 amol corresponds to 2.7% of a full monolayer.

Electrocatalysis. In general, electrocatalysis is performed under conditions where the catalyst is immobilized on the electrode and the substrate is in solution.[54–56] However, in the system described here, the scenario is essentially reversed and the substrate (guanine in DNA) is immobilized on the electrode and the catalyst ($Ru(bpy)_3^{2+}$) is dissolved in the solution. The observations that repeated scanning gives lower currents suggests that the catalytic reaction consumes a large amount of the immobilized DNA in the early times of the reaction. Further, the chronoamperometry data in Figure 2B show that the majority of the catalysis is over within the first 30 ms, which is also consistent with the observation that the catalytic current was easiest to detect by cyclic voltammetry when the scan rate was 10 V/s. These features are in agreement with numerous observations made when both $Ru(bpy)_3^{2+}$ and DNA are in solution, which show that the rate constant for oxidation of guanine by Ru(III) is as high as 10^6 M^{-1} s^{-1}.[28,30,31]

With the low quantities of DNA adsorbed onto the electrode, it is likely that a large fraction of the guanines has been oxidized in a single sweep, which at 10 V/s provides ~60 ms during which there is a significant concentration of Ru(III) at the electrode surface. In fact, roughly 2 electrons/guanine were transferred to the electrode during the cyclic voltammetry experiments. After the adsorbed DNA is consumed, the catalytic cycle does not occur, so large current enhancements are not observed at lower scan rates.

The appeal of a direct electrochemical technique for detecting nucleic acids is that long strands that contain many of the redox-active unit exhibit high responses for individual strands.[4] This concept has been exploited in numerous schemes involving redox chemistry of the DNA bases and recently by Kuhr et al. for oxidation of ribose sugars at copper electrodes.[21] As stated above, the drawback to these direct techniques is that the redox chemistry is either slow or occurs at potentials where the electrode also electrolyzes water. The advantage of the $Ru(bpy)_3^{2+}$-mediated system here is that, like many indirect detection schemes, the electrons are delivered to the electrode by a molecule that exhibits a fast heterogeneous electron transfer. However, the counted electrons originate in the biopolymer, providing some of the advantages of the direct approaches. As in the indirect detection scheme, the ITO electrode exhibits little water oxidation current at the operative potential. At the same time, strands with more guanines give more signal, a point that is well exemplified by Figure 4 and is an advantage typical of direct electrochemistry. This latter point enables subfemtomole detection limits using long DNA strands that contain many oxidizable guanines. Further gains in sensitivity can be effected by miniaturization of the electrode, which could enable the development of a detection scheme for direct analysis of small quantities of nucleic acid derived from biological mixtures.

(48) Thiel, V.; Rashtchian, A.; Herold, J.; Schuster, D. M.; Guan, N.; Siddell, S. G. *Anal. Biochem.* **1997**, *252*, 62–70.
(49) Nooney, M. G.; Campbell, A.; Murrel, T. S.; Lin, X.-F.; Hossner, L. R.; Chusuei, C. C.; Goodman, D. W. *Langmuir* **1998**, *14*, 2750–2755.
(50) Gao, W.; Dickinson, L.; Grozinger, C.; Morin, F. G.; Reven, L. *Langmuir* **1996**, *12*, 6429–6435.
(51) Cao, G.; Hong, H.-G.; Mallouk, T. E. *Acc. Chem. Res.* **1992**, *25*, 420–427.
(52) Hesselink, F. T. In *Adsorption from Solution at the Solid/Liquid Interface*; Parfitt, G. D., Rochester, C. H., Eds.; Academic Press: New York, 1983; pp 377–412.
(53) Stryer, L. *Biochemistry*; 3rd ed.; W. H. Freeman and Co.: New York, 1988.
(54) Glass, A. E. G.; Davis, G.; Francis, G. D.; Hill, H. A. O.; Aston, W. J.; Higgins, I. J.; Plotkin, E. V.; Scott, L. D. L.; Turner, A. P. F. *Anal. Chem.* **1984**, *56*, 667–671.
(55) Kenausis, G.; Chen, Q.; Heller, A. *Anal. Chem.* **1997**, *69*, 1054–1060.
(56) Wilkins, E.; Atanasov, P. *Med. Eng. Phys.* **1996**, *18*, 273–288.

ACKNOWLEDGMENT

We thank the Department of Defense and Xanthon, Inc. for support of this research. Helpful discussions with Drs. Carole Golden, Mary Napier, Patty Ropp, Natasha Popovich, and Allen Eckhardt are gratefully acknowledged.

Received for review January 12, 2000. Accepted June 5, 2000.

AC000051E